



## STATISTICAL DATA ANALYSIS OF GAMMA-RAY BACKGROUND SPECTRA FOR QUALITY ASSURANCE PURPOSES

\*M. WASIM and M. ARIF

Chemistry Division, Directorate of Science, PINSTECH, P.O. Nilore, Islamabad, Pakistan

(Received January 07, 2010 and accepted in revised form February 09, 2010)

Twenty five gamma-ray spectra were accumulated in the gamma-ray spectrometry laboratory located at the Chemistry Division, PINSTECH, Islamabad over a period of three years. Different background components along with their variation with time have been discussed in this paper. It was found that natural component of the background radiations can be reduced with a better design of shielding around the detector. However, the component from the fission products cannot be reduced by increased shielding but with a better shielding material containing less or no fission products.

**Keywords :** Gamma-ray background, Gamma-ray detector shielding

### 1. Introduction

The gamma-ray spectrometry laboratory at the Chemistry Division, Pakistan Institute of Nuclear Science & Technology (PINSTECH), Islamabad, is involved in a number of applications, most of which are related to the characterization of various materials using neutron activation analysis [1-3] and some are related to radiological measurements [4]. The knowledge of background gamma radiation is always important in gamma spectrometry. Although, Compton continuum is also considered as background, but in this work we have restricted ourselves to the non-Compton background only [5]. By background we mean any gamma-rays that do not arise from the sample under investigation *i.e.*, it is not part of the system but part of the surrounding. All processes are subject to some kind of variability, the same is true for  $\gamma$ -ray background. The nature of the background varies greatly with the size and type of detector and with the extent of shielding that may be placed around it [6]. Alongwith other characteristics of the detection system, the detector background also plays an important role in determining the analytical sensitivity of the spectrometer. The lower the background, the better is the analytical sensitivity. The detection limit is also affected by the presence of background, which must be as low as possible especially in the measurement of environmental

radioactivity. Hence, it is important to strive for lower background, although it is usually a tedious process. Room-background is always present and many researchers have studied room background in the past. Some researchers, especially those who are interested in low-background gamma-ray spectrometry, have performed the most detailed studies. Nunez-Lagos and Virto [7] describe a very good and thorough study of room background. Furthermore, background conditions are different at different experimental locations. There are, however, a lot of similarities between them, so it is worthwhile to present our knowledge about our local background conditions. Background identification is also important from the nuclide identification (NID) point of view because proper background subtraction will remove several nuclides, making the NID process computationally less intensive and more accurate. Background radiations are usually grouped into three categories.

1. Natural radioactivity of the constituent materials near the detector
2. Anthropogenic radionuclides from fall out of atmospheric nuclear tests and reactor accidents
3. The primary and secondary components of cosmic radiations

There are around twenty singly occurring primordial radionuclides, among them some have

\*Corresponding author : wasim1968@gmail.com

very long half lives and some are beta or alpha emitters [8].  $^{40}\text{K}$  is the only suitable singly occurring primordial radionuclide, which is readily detectable by  $\gamma$ -ray spectrometry. Other radionuclides of terrestrial origin are characterized in terms of radioactive series. Most of the radionuclides identified in a  $\gamma$ -ray spectrum are from two series, one starting with  $^{238}\text{U}$  and the other with  $^{232}\text{Th}$ .  $^{238}\text{U}$  and  $^{232}\text{Th}$  both are present in most of crustal rocks [9, 10]. Since  $^{238}\text{U}$  and  $^{232}\text{Th}$  both emit very weak  $\gamma$  lines, they are estimated by the presence of their progenies in their decay series. The background radiation rate, although expected to be nearly steady state in time, may show perceptible variation over periods of hours or days [11]. A measurable amount of background can originate with radioactivity carried by ambient air, either in the form of trace amounts of radioactive gases or dust particles. The radionuclides  $^{222}\text{Rn}$  and  $^{220}\text{Rn}$  are short-lived radioactive gases that originate as daughter products in the decay chains of uranium and thorium present either in the soil or in construction materials of the laboratory. Their concentrations in the atmosphere can vary significantly depending on the time of day and meteorological conditions. To eliminate the influence of radon on the background, the volume around the detector can be made airtight and purged with a radon-free gas. Some laboratories use boil-off nitrogen gas from a liquid nitrogen dewar for this purpose. Much of the observed variation in sensitive gamma-ray counters appears to be correlated with airborne activity in the form of decay products of  $^{222}\text{Rn}$ . In low-level counting experiments, it is therefore imperative to carry out a background determination near the time of the actual measurement itself.

Anthropogenic radionuclides known as fission products originating from past nuclear tests conducted in the atmosphere from 1948-1969 and from nuclear accidents are widely distributed in the environment. Among these radionuclides, the most prominent contributor is  $^{137}\text{Cs}$  but amounts of  $^{95}\text{Zr}$ ,  $^{95}\text{Nb}$ ,  $^{106}\text{Ru}$ ,  $^{125}\text{Sb}$ ,  $^{144}\text{Ce}$  and  $^{60}\text{Co}$  can also be detected [6].  $^{137}\text{Cs}$  with a long half life ( $\sim 30$  y) and high fission yield was released in the atmosphere in large quantities in nuclear tests. Its concentration varies due to re-suspension of soil [12]. The Southern Hemisphere has remained relatively free of  $^{137}\text{Cs}$ . The deposition in both hemispheres is highest at midlatitude and decreases on moving towards the poles or the

equator. With the exception of local contamination due to reactor accidents  $^{137}\text{Cs}$  is virtually undetectable in the atmosphere of Southern Hemisphere [13].

Cosmic radiations are primary radiations of very high energy (upto  $10^8$ - $10^9$  GeV) that originate in outer space and impinge isotropically on the top of the earth's atmosphere. These particles undergo collisions in the stratosphere and give rise to mesons, muons, neutrinos, electrons, neutrons and protons. Among these 87% are protons, 11%  $\alpha$  particles, about 1% nuclei of atomic number  $Z$  between 4 and 26, and about 1% electrons of very high energy [14]. The interactions of the primary particles with atmospheric nuclei produce electrons,  $\gamma$  rays, neutrons and mesons. The interesting cosmic rays secondaries for background considerations are only muons and neutrons. At sea level, fluxes of protons, electrons, neutrons and muons are in the proportion 1/26/37/111 [15] with a flux of  $1.7 \text{ m}^{-2} \text{ s}^{-1}$  for protons. Neutron induced background pulses in high  $Z$  materials (Ge, Pb, Fe, Cu etc) give rise to fast neutrons. They are characterized by different nuclear reactions, which generate discrete  $\gamma$  lines. Most of the currently observed  $\gamma$ -rays are due to  $(n, n')$  reactions. Fast neutrons can also be slowed down giving cosmic rays induced thermal fluxes of typically  $10^{-3}$  to  $3 \times 10^{-3} \text{ cm}^{-2} \text{ s}^{-1}$ . Thermal neutrons contribute to the background via activation process essentially in the high purity germanium (HPGe) detector itself.

The main theme of this paper is to identify the background components in our gamma-ray spectrometry laboratory and to explore different statistical tools for the assessment of background spectra. These tools will be applied for quality control in our gamma-ray measurements.

## 2. Experimental

Our laboratory where all background spectra were acquired has the dimension of  $12.5 \times 15.2 \times 9 \text{ ft}^3$ ; with two walls of brick and the other two walls made of wooden sheet and glass, the roof and floor are made of concrete. The laboratory is equipped with a p-type coaxial HPGe detector (Eurisy Mesures, France). The sensitive volume of the detector is  $245 \text{ cm}^3$  with dead layer of  $500 \mu\text{Ge}$  and length 70 mm, external diameter 67.5 mm having entrance window of Al with thickness  $\leq 1$

mm. The detector has 60% relative efficiency and 1.95 FWHM at 1332 keV. It is connected to an Ortec-570 amplifier and Trump PCI 8k ADC/MCA card with GammaVision-32 version 6 software. The detector shielding is made up of lead in the form of cylindrical rings of total length 40.5 cm, with a hole inside to house the detector crystal. The wall thickness of cylinder is 5.5 cm. There is no internal lining on the lead shields. The detector shielding with housing is shown in Figure 1.

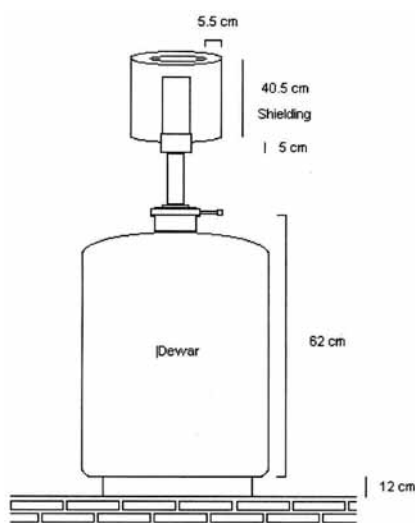


Figure 1. Housing of HPGe detector with shielding, the dimensions are not to the scale.

### 3. Results and Discussion

All calculations, in this study, have been made in Microsoft Excel and by computer programs written in MATLAB by the authors of this paper. The data presented in this paper corresponds to the 25 background spectra acquired from 10-Feb-2006 to 13-Aug-2009. All spectra were assigned numbers from 1 to 25 in chronological order. The number of peaks observed in 25 spectra varies from a minimum of 37 to maximum of 81 and with 59 as the average. The acquisition time varied from 11 hours to 91 hours. The data analysis shows that the increase in the number of peaks is insignificant after 24 hours of acquisition time.

The data in Table 1 shows five types of radionuclides identified in the laboratory background; these include natural, cosmic, contaminants, fission products and reactor release. The radionuclides  $^{228}\text{Ac}$ ,  $^{212}\text{Bi}$ ,  $^{214}\text{Bi}$ ,  $^{234\text{m}}\text{Pa}$ ,  $^{212}\text{Pb}$ ,  $^{214}\text{Pb}$ ,  $^{226}\text{Ra}$ ,  $^{208}\text{Tl}$  and  $^{40}\text{K}$  belong to the "Natural" category,  $^{75\text{m}}\text{Ge}$  is a "Cosmic"

radionuclide,  $^{152}\text{Eu}$ ,  $^{154}\text{Eu}$  and  $^{134}\text{Cs}$  are the "Contaminants" near the detector,  $^{60}\text{Co}$  and  $^{137}\text{Cs}$  are from previous nuclear explosions or accidents ("Fission Products") and  $^{41}\text{Ar}$  is "Release" from the research reactor which has been reported earlier [17]. Table 1 also shows the most prominent peak of each radionuclide with the average CPS and limit of detection (LoD) based on the average CPS. In case when there is a contribution of background, then LoD is calculated as:

$$\text{LoD} = 3\sigma_{\text{cps}} \quad (1)$$

Where

$$\sigma_{\text{cps}} = \frac{\sqrt{A_{\text{BG}}}}{t_{\text{BG}}} \quad (2)$$

where  $A_{\text{BG}}$  is peak area in the background and  $t_{\text{BG}}$  is counting time of background. The CPS and LoD data is based on the last 8 background spectra for the reason described in later sections. Amongst all,  $^{41}\text{Ar}$  has been observed with the highest count rate followed by Pb x-rays,  $^{40}\text{K}$ ,  $^{152}\text{Eu}$ ,  $^{134}\text{Cs}$ ,  $^{214}\text{Bi}$ ,  $^{214}\text{Pb}$ ,  $^{212}\text{Pb}$ ,  $^{154}\text{Eu}$  and other radionuclides. This pattern is presented in Figure 2, which shows average CPS of last 8 background spectra. This pattern shows that the activity concentrations of the radionuclides originating from  $^{238}\text{U}$  series are more prominent than those produced by the  $^{232}\text{Th}$  series.

Figure 3 shows variation of total count rate of spectra 5 to 25 with the counting date. As the first four spectra were recorded using different shielding schemes for each acquisition therefore this data is not included in further analysis. In Figure 3, three peaks can be located in the data denoted by  $\times$ , which correspond to the emission of  $^{41}\text{Ar}$  from Pakistan Research Reactor (PARR-1), a 10 MW research reactor, thus increasing the total count rate. Apart from the spectra containing  $^{41}\text{Ar}$ , three different regions can be observed in Figure 3 corresponding to three different shielding schemes, namely: region-1 which includes spectra 5-8 and 11, region-2 containing spectra 12-16 and region-3 comprises of spectra 20-23 and 25. The shielding scheme-1 corresponding to the region-1 was constituted of lead bricks around the detector. Whereas the region-2 corresponds to shielding scheme-2 which was comprised of 3 lead rings put one upon the other vertically around the detector. The region-3 corresponding to shielding scheme -3

Table 1. Listing and identification of room-background gamma radiation at the NAA Laboratory.

NID	No. of Spectra	Source	Most common peaks		
			Peak Energy (keV)	Average CPS	LoD (CPS)
Pb (x-rays)	25	Natural ( $^{238}\text{U}$ , $^{232}\text{Th}$ )	75.0	0.187	-
			72.8	0.106	
			85.0	0.093	
			87.4	0.029	
$^{234}\text{Th}$	24	Natural ( $^{238}\text{U}$ )	92.7	0.011	0.0013
$^{234\text{m}}\text{Pa}$	6	Natural ( $^{238}\text{U}$ )	98.3	0.010	0.0013
			1001.2	0.002	0.0006
$^{226}\text{Ra}$	24	Natural ( $^{238}\text{U}$ )	185.9	0.008	0.0011
$^{214}\text{Pb}$	23	Natural ( $^{238}\text{U}$ )	351.9	0.015	0.0015
			295.3	0.009	0.0012
			241.8	0.003	0.0007
$^{214}\text{Bi}$	25	Natural ( $^{238}\text{U}$ )	609.2	0.019	0.0017
			1120.6	0.012	0.0014
			1238.5	0.005	0.0009
			1764.9	0.019	0.0017
$^{228}\text{Ac}$	25	Natural ( $^{232}\text{Th}$ )	338.4	0.004	0.0008
			911.4	0.012	0.0014
$^{212}\text{Pb}$	25	Natural ( $^{232}\text{Th}$ )	238.7	0.013	0.0014
$^{212}\text{Bi}$	17	Natural ( $^{232}\text{Th}$ )	1621.2	0.001	0.0005
$^{208}\text{Tl}$	24	Natural ( $^{232}\text{Th}$ )	583.2	0.009	0.0012
			282.0	0.009	0.0012
$^{40}\text{K}$	25	Natural	1461.3	0.095	0.0038
$^{75\text{m}}\text{Ge}$	6	Cosmic	140.4	0.010	0.0013
$^{152}\text{Eu}$	25	Contaminant	121.8	0.098	0.0039
			244.7	0.018	0.0017
			344.3	0.067	0.0032
			779.1	0.021	0.0018
			1086.1	0.016	0.0016
			1112.2	0.022	0.0018
$^{154}\text{Eu}$	25	Contaminant	123.1	0.013	0.0014
			248.0	0.009	0.0012
$^{134}\text{Cs}$	17	Contaminant	604.7	0.045	0.0027
			795.5	0.029	0.0021
$^{137}\text{Cs}$	21	Fission product	661.8	0.005	0.0009
$^{60}\text{Co}$	25	Fission product	1173.5	0.008	0.0011
			1332.9	0.009	0.0012
$^{41}\text{Ar}$	8	Reactor release	1293.7	2.110	-

used 6 lead rings in a design similar to scheme-2. The three regions show different average count rates; the region-1 has an average of 20.9, region-2 has 13.2 and region-3 has 11.4 CPS, which supports the argument that each shielding scheme was better than its predecessors. Similar behaviour can be seen with more clarity in Figure 4, which depicts variation of count rate of 911.4 keV peak of  $^{228}\text{Ac}$ . This figure shows three distinct

regions, with a decrease in count rate for every new shielding arrangement. The similar behaviour is observed with all other natural radionuclides

The count rate variation of the peaks of  $^{41}\text{Ar}$ ,  $^{60}\text{Co}$  and  $^{137}\text{Cs}$  was found to be random, which is different from the variation patterns depicted by natural radionuclides. The count rate variation of  $^{41}\text{Ar}$  is totally independent of shielding design since

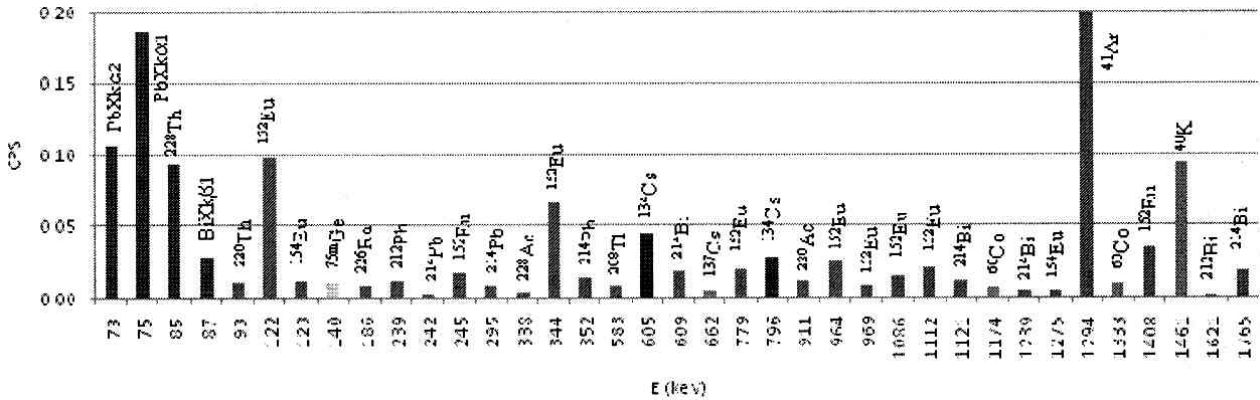


Figure 2. A plot of highest cps for each radionuclide.

this noble gas approaches the detector from various pathways. The count rate variation of  $^{60}\text{Co}$  and  $^{137}\text{Cs}$  shows that these radionuclides are not affected by shielding design, which means that these radionuclides are present in many objects including the shielding. The variation of peak count rate of  $^{137}\text{Cs}$  has been shown in Figure 5. The  $^{75\text{m}}\text{Ge}$  peak was observed only in 6 spectra thus provides little information to discuss its behaviour.

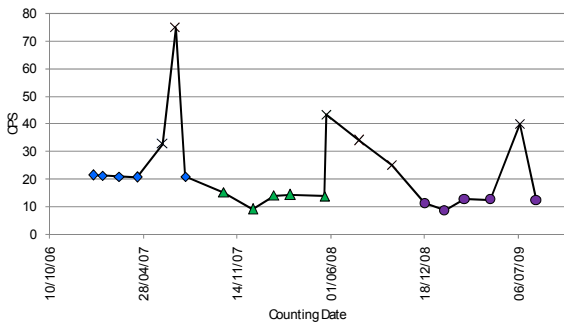


Figure 3. Variation of total counts rate (CPS) with time.

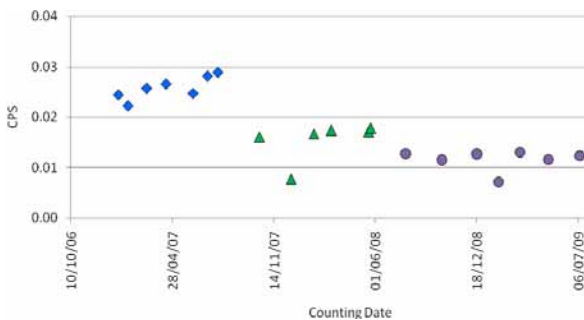


Figure 4. Variation of counts rate (CPS) of 911.4 keV peak of  $^{228}\text{Ac}$ , showing 3 separate regions.

To investigate the behaviour of contaminants, a comparison has been presented in Figure 6

between count rate of spectra 5-25 of the 911 keV peak of  $^{228}\text{Ac}$  (Natural) with 1408 keV peak of  $^{152}\text{Eu}$  and 795 keV peak of  $^{134}\text{Cs}$ . Since  $^{152}\text{Eu}$  and  $^{154}\text{Eu}$  are produced together as activation products we assume the same behaviour for both radionuclide and will not discuss  $^{154}\text{Eu}$  separately. The correlation coefficient between the count rates of spectra 1 to 25 of  $^{152}\text{Eu}$  and  $^{228}\text{Ac}$  is 0.595, which shows a significant correlation at 95% confidence level. This indicates that the implementation of a new shielding scheme, after first 11 spectra, lowered the detector background due to both natural radiation as well as contaminants. If the correlation is calculated again removing the first 11 data points in both data sets, the correlation becomes 0.139, which is insignificant at 95% confidence level, showing that contaminants behave differently as compared to the natural products. It is clear in Figure 6 that the last 4 points have an increased count rates for  $^{152}\text{Eu}$  and  $^{134}\text{Cs}$ , which means that after 31-Jan-2009 new contamination took place around the detector. The increase in count rate is not proportional in  $^{152}\text{Eu}$  and  $^{134}\text{Cs}$ ; the increase in count rate of  $^{134}\text{Cs}$  is ten fold and that of  $^{152}\text{Eu}$  is two fold.

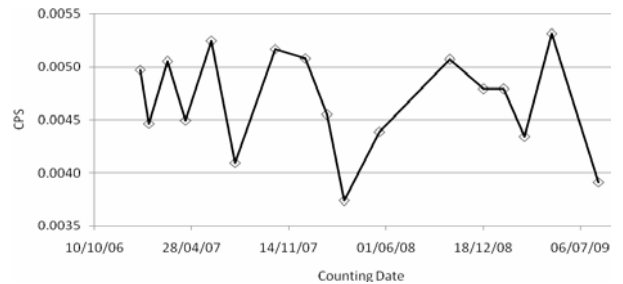


Figure 5. Variation of counts rate (CPS) of 661.6 keV peak of  $^{137}\text{Cs}$ , showing random distribution.

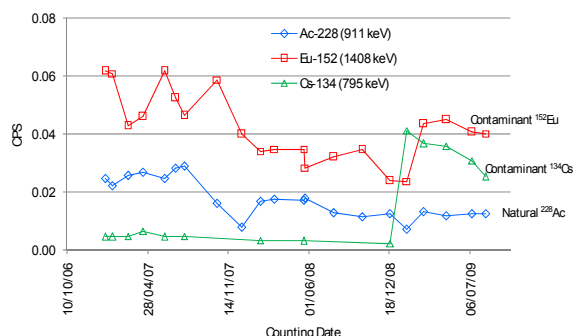


Figure 6. A comparison of count rates of 1408 keV peak of  $^{152}\text{Eu}$ , 795 keV peak of  $^{134}\text{Cs}$  and 911 keV peak of  $^{228}\text{Ac}$ .

Background correction is an important step in the activity calculations. The best strategy for background correction is to subtract the background which should be taken close to time of sample acquisition, provided there was no change in the shielding scheme. A good quality assurance program needs the regular record of several parameters [18], one of which is the background spectra. Furthermore, control charts of background help rapidly identify any change and its removal can be performed. In the implementation of quality control, the determination of the following factors will prove helpful.

1. Total count rate, which will provide information whether  $^{41}\text{Ar}$  was part of the background or not.
2. Identification of radionuclides and their comparison with those previously detected to identify new contamination.
3. Determination of count rate of a peak from natural, contaminants ( $^{152}\text{Eu}$ ,  $^{134}\text{Cs}$  etc) and fission products ( $^{137}\text{Cs}$ ).

#### 4. Conclusions

One of the main aims in background recording is to find out any contamination around the detector. Although the record of total count rate is important but it does not tell anything about the presence of contaminants due to statistical variation in the total count rate under normal background. The detection of all nuclides, their comparison with the previously recorded data and a comparison of natural, contaminants and fission products count rate is necessary for quality assurance purposes. A laboratory's background sets the limit of detection in radiological measurements as well as in neutron activation analysis. Therefore, the system's sensitivity can be monitored by regular measurement of the detector background.

#### References

- [1] M. Wasim, J. H. Zaidi, M. Arif and I. Fatima, *J. Radioanal. Nucl. Chem.* **277** (2008) 525.
- [2] M. Wasim, M. Arif, J. H. Zaidi and I. Fatima, *Radiochim. Acta* **96** (2008) 863.
- [3] M. Wasim, M. Arif, J.H. Zaidi and Y. Anwar, *Radiochim. Acta* **97** (2009) 651.
- [4] I. Fatima, J. H. Zaidi, M. Arif, M. Daud, S.A. Ahmad and S. N. A. Tahir, *Radiat. Prot. Dosim.* **128** (2008) 206.
- [5] T. Belgya, Zs. Revay and G. L. Molnar, *J. Radioanal. Nucl. Chem.* **265** (2005) 181.
- [6] G. F. Knoll, *Radiation Detection and Measurement*, 3rd Ed. John Wiley & Sons (2000).
- [7] R. Nunez-Lagos and A. Virto, *Appl. Radiat. Isot.* **47** (1996) 1011.
- [8] R. L. Kathren, *Appl. Radiat. Isot.* **49** (1998) 149.
- [9] United Nations Scientific Committee on the Effects of Atomic Radiation, Publication E.82.IX.8, United Nations, New York (1982).
- [10] National Council on Radiation Protection and Measurements, *Measurement of Radon Daughters in Air*, NCRP Report 97, Bethesda (1988).
- [11] S. S. Al-Dargazelli, A. H. Al-Bayati and R. S. Jaboori, *J. Radioanal. Nucl. Chem. Art.* **131** (1989) 223.
- [12] S. R. Biegalski, B. Hosticka and L. R. Mason, *J. Radioanal. Nucl. Chem.* **248** (2001) 643.
- [13] M. A. Pires Do Rio, E. C. S. Amaral and H. G. Paretzke, *J. Aerosol Sci.* **25** (1994) 821.
- [14] National Council on Radiation Protection and Measurements, *Natural Background Radiation in the United States*, NCRP Rep. No. 45, Bethesda, Maryland (1975).
- [15] G. Heusser, *Proceedings of the 3rd Int. Summer School on Low Level Measurements of Radioactivity in the Environment*, Huelva, Spain (1993) pp. 63-112.
- [16] R.M. Lindstrom, D.J. Lindstrom, L.A. Slaback and J.K. Langland, *Nucl. Instr. & Meth. A* **299** (1990) 425.
- [17] M. Wasim, J. H. Zaidi, M. Arif and Y. Anwar, *The Nucleus* **46** (2009) 495.
- [18] M. Wasim, *J. Radioanal. Nucl. Chem.* **272** (2007) 61.